Rev.Adv.Mater.Sci. 18(2008) 121-125

MICROSTRUCTURE EXAMINATION OF THE $Zr_{65}Al_{10}Ni_{10}Cu_{15}$ BULK METALLIC GLASS AFTER SUPERPLASTIC GAS-PRESSURE FORMING

H.G. Jeong[1] and W.J. Kim[2]

[1]Digital Production Processing and Forming Team, Manufacturing Process Research Division, Korea Institute of Industrial Technology, 994-32, Dongchon-dong, Yeonsu-gu, Incheon Metropolitan City 406-130, Korea
[2]Department of Materials Science & Engineering, Hong-Ik University,72-1, Sangsu-dong, Mapo-ku, Seoul 121-791, Korea

Received: March 29, 2009

Abstract. Microstructure and crystallinity during superplastic gas-pressure forming of the $Zr_{65}Al_{10}Ni_{10}Cu_{15}$ bulk metallic glass sheet fabricated by squeeze copper-mold casting method was examined. A small degree of crystallization (5.7~8.7 vol.%) was found to occur during the forming, though the sum of heating and holding time for the sample and forming time was controlled to be much less than the onset time of crystallization predicted by the T.T.T diagram of the metallic glass sheet. The degree of crystallization depended on position of the deformed body, which was highest at the apex where the largest straining took place, indicating acceleration of crystallization kinetics assisted by plastic flow. The strain-rate-change test at 696K performed in tension repeated for four times consecutively on a given sample suggested that superplastic-flow behavior of the metallic glass sheet would not have been significantly affected by crystallization during hot gas-blow forming.

1. INTRODUCTION

Superplastic formability of bulk metallic glass (BMG) allows to fabricate near-net-shape of macro and micro components with superior mechanical and corrosion-resistant properties. The superplasticity in metallic glasses is typically observed in a specific temperature range so called supercooled liquid region defined by the difference between glass transition temperature (T_g) and crystallization temperature (T_x) [1-4]. In the previous work, superplastic behavior of the $Zr_{65}Al_{10}Ni_{10}Cu_{15}$ bulk metallic glass sheet produced by a squeeze copper-mold casting method was studied under gas-pressure [5]. A hemisphere could be successfully formed when the forming procedures were properly controlled. In this paper, microstructure and crystallinity of the superplastically deformed $Zr_{65}Al_{10}Ni_{10}Cu_{15}$ sheet by gas pressure was examined and the result was discussed.

2. EXPERIMENTAL PROCEDURES

The $Zr_{65}Al_{10}Ni_{10}Cu_{15}$ alloy ingot was prepared by arc-melting the mixture of pure Zr, Al, Ni, and Cu metals in pure argon atmosphere. From complete remelting of the alloy ingot in the arc furnace, a sheet sample 65 mm long, 40 mm wide, and 1 mm thick was fabricated by using squeeze copper-mold casting. The cast sheet was confirmed to be fully amorphous [5]. A diaphragm with a 22 mm diameter was cut from a part of the sheet squeeze-formed on the copper mold, trimmed and then surface-grinding treated on its both sides to a thickness of 0.8 mm.

Corresponding author: W.J. Kim, e-mail: kimwj@wow.hongik.ac.kr

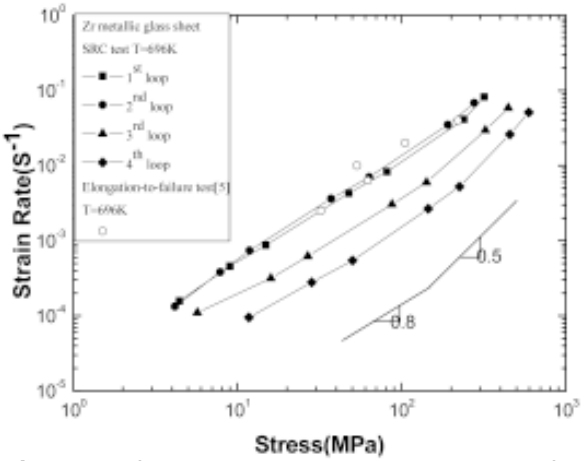

Fig. 1. Strain rate vs. stress curves at 696K. The test was repeated four times consecutively on a given sample.

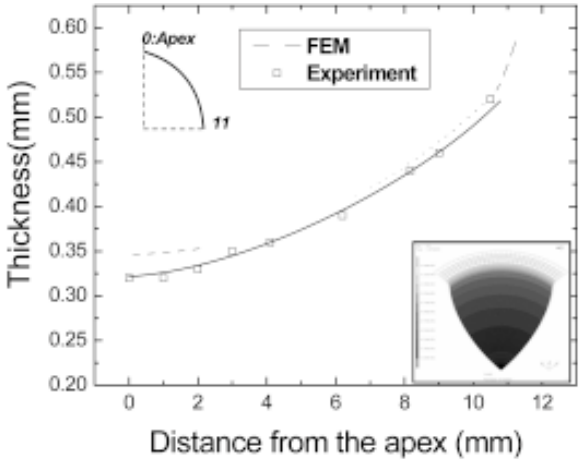

Fig. 2. Comparison in thickness distribution between the FEM and experimental results [5].

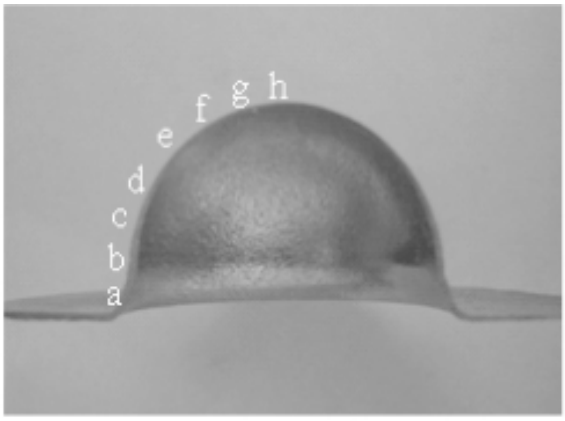

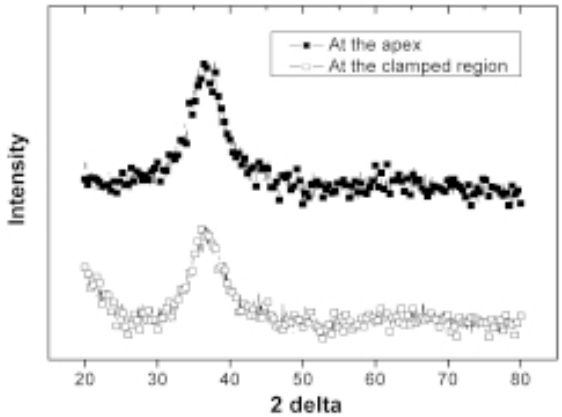

Fig. 3. (a) The sample formed by gas blow at 696K (b) XRD tests at the apex and clamped regions on the deformed body.

Gas forming was performed at 696K in N_2 atmosphere following the gas-pressure schedule calculated by finite element method (FEM). To minimize the possibility of crystallization during the forming, the upper and lower dies (blank holder) were preheated at the target temperature of 696K without the sample. After the sample was mounted on the die, a heating plus holding time less than 200 s was applied and then a forming time of 120 s was given for complete filling into the die. More detailed procedure for the gas blow forming is available elsewhere [5]. Crystallinity during the deformation was examined using X-ray diffraction (XRD), transmission electron microscopy (TEM) and differential scanning calorimeter (DSC). Strain rate change (SRC) test was performed 696K to investigate variation of the strain rate sensitivity exponent, *m*, and flow stress during plastic flow. The test was repeated four times consecutively on a given sample where a true strain of 0.2~0.3 was consumed during each loop.

3. RESULTS AND DISCUSSION

Fig. 1 shows that the strain rate–stress curves obtained from the SRC test after the fourth loop. The figure shows that the curves little altered during the first and second loops but notably changed in slope and flow stress during the third and fourth loops. Crystallization is most likely responsible for the change. The strain rate sensitivity exponent, *m*, could be determined from the strain rate–stress curves as inverse of the slope (=1/*n*, where *n* is the stress exponent representing the slope). During the first and second loops, the *m* value was measured to be 0.8 in most of the strain rate range covered in the present study except the high strain

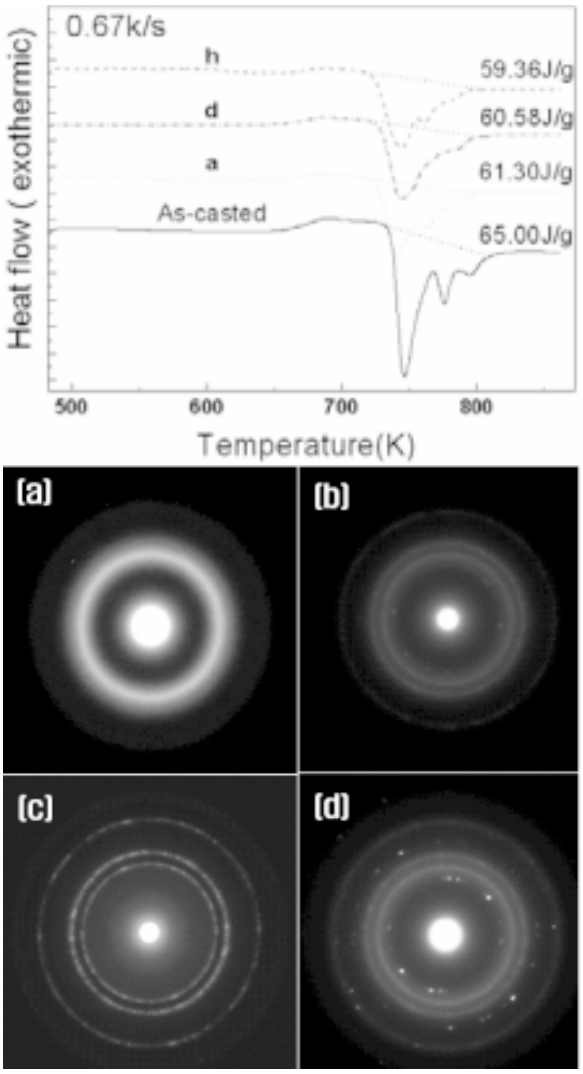

Fig. 4. (a) DSC curves and (b) SAED patterns at different sampling points on the deformed hemisphere [a] as-cast sheet, [b] a region, [c] d region and [d] h region, respectively.

rates above $3.5 \cdot 10^{-2}$ s^{-1} where m=0.5 is associated. It is worthy to note that the elongation-to-failure data [6] show a good overlap on the SRC curves for the first and second loops. The m values measured in low and high strain rate ranges did not change notably in the subsequent (third and fourth) loops, but the critical strain rate associated with the slope transition from low to high tended to decrease with increasing number of loop. It was lowered to $6 \cdot 10^{-3}$ s^{-1} and $5 \cdot 10^{-3}$ s^{-1} from $3.5 \cdot 10^{-2}$ s^{-1} during the third and fourth loops, respectively. Another important observation to note was the large increase in flow stress during the third and fourth loops. For example, the flow stress at $5 \cdot 10^{-3}$ s^{-1}(the target strain rate), which was 52 MPa during the first and second loops, drastically increased to 129 MPa and 226 MPa during the third and fourth loops, respectively. The volume fractions of crystalline phase just after the second (interrupted) and fourth loops were determined on the gauge regions of the separate samples by measuring the heat release during DSC scanning. They were 7% and 34% (calculated by Eq. (1)), respectively. Therefore, it can be inferred from the current data of the SRC test that as crystallization proceeds, 1) m value decreases, especially at high strain rates, and region the associated with Newtonian viscous flow shrinks and 2) flow stress significantly increases. The decrease of m value and the increase of flow-stress would deteriorate superplasticity and require a higher gas pressure for forming, respectively.

After the blow forming, the deformed product was cut into two parts in the diameter to measure thickness distribution. The thickness profile of the hemisphere is shown in Fig. 2. Thickness was minimum at the apex (0.35 mm) where the corresponding strain was 0.82. Thickness along the periphery increased toward the clamped region. The experimental result was in a reasonable agreement with the FEM result where the constitutive equation determined based on the strain rate-stress curves obtained from the first loop or from the elongation-to-failure data in Fig. 1 was utilized.

Fig. 3a shows the cross section of the hemisphere after the forming. XRD experiments were conducted at the apex (marked as h) and near the clamped region (marked as a) on the hemisphere component to check possible occurrence of crystallization during the forming process. Absence of distinct crystalline peaks was apparent at both places (Fig. 3b), indicating that the sheet remained (almost) fully amorphous after the forming.

For more careful examining of the possibility of crystallization, a series of DSC and selected-area electron diffraction (SAED) analyses by TEM were performed on the deformed sample and the results are shown in Figs. 4 and 5, respectively. For all the sampling points on the deformed sample, the heat of crystallization was less than that of the as-cast sample and it tended to decrease as the point moves toward the apex (Fig. 4a). The overall amount of the crystallized phase was estimated by measuring the amount of heat flow, ΔH_x, from the DSC curves. By knowing the ΔH_x and ΔH_{bx} (=the heat of crystallization of the as-received material) values, the volume fraction of crystalline phases

Table 1. DSC data of the sampling points on the deformed body.

Sample	T_g(K)	T_x(K)		ΔT_x	ΔH	V_{cry}
		T_{x1}	T_{x2}	(=T_{x1}- T_{x2})	(J/g)	
As-cast	668.20	737.59	746.73	69.39	65.0	0
h	663.91	725.07	743.97	61.16	59.36	8.7
d	664.02	729.70	743.86	65.68	60.58	6.8
a	661.38	727.56	741.05	66.18	61.3	5.7

(V_{cry}) could be calculated based on the following relation;

$$_{cry} = \frac{\Delta H_{bx} - \Delta H_x}{\Delta H_x} \times 100(\%). \quad (1)$$

At the apex region (marked as h) associated with the largest deformation, the volume fraction of crystalline phase was highest as 8.6%. It was lowest as 5.7% at the clamped region (marked as a) associated with the smallest deformation. The detailed information regarding the DSC results is provided in Table 1.

The estimation of volume fraction of crystalline phase by measuring the heat release during DSC scan agrees with the corresponding SAED patterns shown in Fig. 4b, which are composed of spotty diffraction rings with a diffuse background from the amorphous matrix, indicating occurrence of a small degree of crystallization at entire regions but the highest degree of crystallization at the apex region where many number of diffraction spots from crystalline particles are observed.

High resolution TEM micrographs of the as-cast and the apex region on the deformed hemisphere are shown in Fig. 5. In comparison with the microstructure of the as-cast sheet, formation of nano-sized crystals is obvious at the apex region. The above DSC and TEM results clearly show that some degree of crystallization took place under the current forming condition despite the effort of minimizing the sample heating and holding time and forming time to avoid crystallization. That is, crystallization took place though time consumption during the forming test (320 s) was much less than that predicted by the T.T.T. diagram (1700 s) [6,7]. It is believed that this premature crystallization is related to nature of crystallization acceleration by plastic flow. In fact, it was reported previously on the same alloy system that crystallization reaction

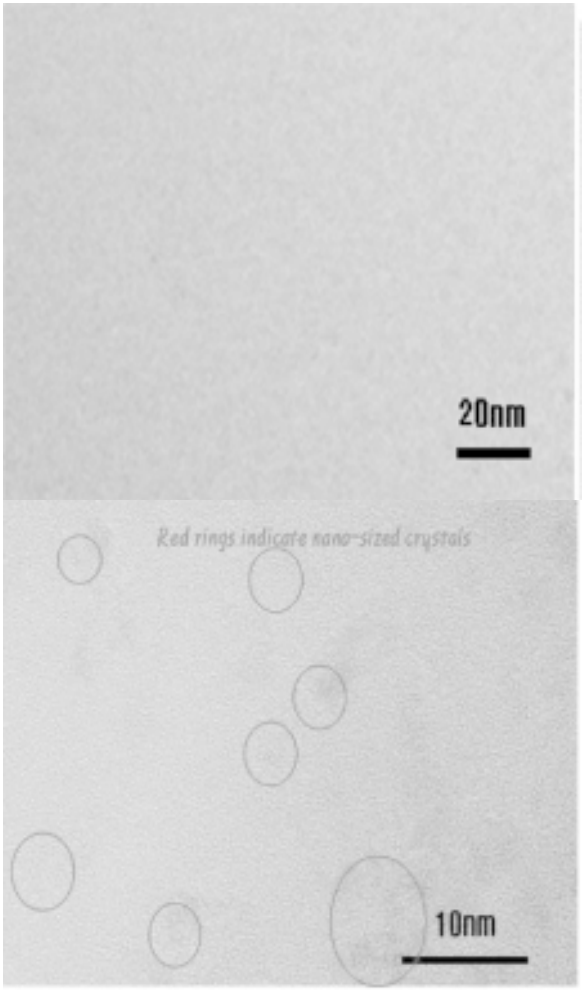

Fig. 5. HRTEM micrographs of (a) the as-cast sheet and (b) the apex region of the deformed hemisphere.

percentage at the deformed section was considerably larger than that at the undeformed section

when the gauge and grip regions of a sample pulled in tension was examined [7].

It is worthwhile to note that the volume fraction of crystalline phase measured at the apex (8.7%) is close to that measured after the second loop in the SRC test (7%) up to which no visible changes in *m* value and flow stress were detected. For this reason, it can be concluded that the plastic flow behavior during gas-blow-forming was little affected by crystallization under the current experimental condition, though some crystallization took place. The agreement in thickness distribution between the experimental and FEM results also proves this point.

To reduce the extent of crystallization during forming, shorter holding time and higher strain rate may need to be considered and this issue is currently in study.

4. SUMMARY

Microstructure and crystallinity of the hemisphere-shape product of $Zr_{65}Al_{10}Ni_{10}Cu_{15}$ BMG fabricated by gas blow forming at 696K was examined. The DSC and TEM analysis revealed that some crystallization took place during the forming though the time consumed for the forming processing was significantly less than the onset time of crystallization predicted by the T.T.T. diagram. The degree of crystallization was highest at the apex region where the largest deformation took place. Acceleration of crystallization kinetics by plastic flow was the cause. The results from the strain rate change test in tension at 696K indicate that as crystallization proceeds, *m* value decreases, especially at high strain rates and flow stress largely increases. The volume fraction of crystalline phase measured at the apex (8.7%) was found to be low enough for plastic flow of the material to be affected by crystallization during the gas-blow forming.

ACKNOWLEDGEMENT

This work was financially supported by MOCIE (Ministry of Commerce, Industry and energy) under the project named as development of structural metallic materials and parts with the super strength and high performance.

REFERENCES

[1] A. Inoue, H.M. Kimura, K. Sasamori and T. Masumoto // *Mater Trans JIM* **35** (1994) 85.
[2] C.C. Hays, C.P. Kim and W.L. Johnson // *Phys Rev Lett* **84** (2000) 2901.
[3] K. Hashimoto, *Current topics in amorphous materials*, In: *Physics and technology*, ed. by Y. Sakurai, Y. Hamakawa, T. Masumoto, K. Shirae and K. Suzuki (Elsevier, Amsterdam, 1993), p. 167.
[4] Y. Kawamura, V. Shibata, A. Inoue and T. Masumoto // *Appl Phys Lett* **69** (1996) 1208.
[5] W.J. Kim, J.B. Lee and H.G. Jeong // *Materials Science and Engineering: A* **428** (2006) 205.
[6] W.J. Kim, Y.K. Sa, J.B. Lee and H.G. Jeong // *Intermetallics* **14** (2006) 377.
[7] W. J. Kim, D. S. Ma and H. G. Jeong // *Scripta Materialia* **49** (2003) 1067.